OPEN ACCESS Freely available online

PLoS PATHOGENS

The Tripartite Associations between Bacteriophage, *Wolbachia,* and Arthropods

Seth R. Bordenstein*, Michelle L. Marshall, Adam J. Fry¤, Ulandt Kim, Jennifer J. Wernegreen

Josephine Bay Paul Center for Comparative Molecular Biology and Evolution, The Marine Biological Laboratory, Woods Hole, Massachusetts, United States of America

By manipulating arthropod reproduction worldwide, the heritable endosymbiont *Wolbachia* has spread to pandemic levels. Little is known about the microbial basis of cytoplasmic incompatibility (CI) except that bacterial densities and percentages of infected sperm cysts associate with incompatibility strength. The recent discovery of a temperate bacteriophage (WO-B) of *Wolbachia* containing ankyrin-encoding genes and virulence factors has led to intensifying debate that bacteriophage WO-B induces CI. However, current hypotheses have not considered the separate roles that lytic and lysogenic phage might have on bacterial fitness and phenotype. Here we describe a set of quantitative approaches to characterize phage densities and its associations with bacterial densities and CI. We enumerated genome copy number of phage WO-B and *Wolbachia* and CI penetrance in supergroup A- and B-infected males of the parasitoid wasp *Nasonia vitripennis*. We report several findings: (1) variability in CI strength for A-infected males is positively associated with bacterial densities, as expected under the bacterial density model of CI, (2) phage and bacterial densities have a significant inverse association, as expected for an active lytic infection, and (3) CI strength and phage densities are inversely related in A-infected males; similarly, males expressing incomplete CI have significantly higher phage densities than males expressing complete CI. Ultrastructural analyses indicate that approximately 12% of the A *Wolbachia* have phage particles, and aggregations of these particles can putatively occur outside the *Wolbachia* cell. Physical interactions were observed between approximately 16% of the *Wolbachia* cells and spermatid tails. The results support a low to moderate frequency of lytic development in *Wolbachia* and an overall negative density relationship between bacteriophage and *Wolbachia*. The findings motivate a novel phage density model of CI in which lytic phage repress *Wolbachia* densities and therefore reproductive parasitism. We conclude that phage, *Wolbachia,* and arthropods form a tripartite symbiotic association in which all three are integral to understanding the biology of this widespread endosymbiosis. Clarifying the roles of lytic and lysogenic phage development in *Wolbachia* biology will effectively structure inquiries into this research topic.

Citation: Bordenstein SR, Marshall ML, Fry AJ, Kim U, Wernegreen JJ (2006) The tripartite associations between bacteriophage, *Wolbachia,* and arthropods. PLoS Pathog 2(5): e43. DOI: 10.1371/journal.ppat.0020043

Introduction

Wolbachia are α–proteobacterial endosymbionts that are recognized for their widespread distribution and inductions of reproductive parasitism, including feminization, male-killing, parthenogenesis, and cytoplasmic incompatibility (CI) in arthropods [1]. The success of these modifications has likely led to the worldwide spread of this maternally transmitted bacterium in at least 20% of all arthropod species [2–4]. Since insects comprise approximately 85% of all animal species, *Wolbachia* are by extrapolation one of the most abundant, obligate intracellular parasites in the biosphere and may affect major evolutionary processes including sexual selection [5], sex determination [6], and speciation [7–10] in their arthropod hosts. Like many maternally transmitted bacteria, *Wolbachia* typically infect the cells of the gonadal tissues.

CI is a common reproductive alteration induced by *Wolbachia* in insects. It is expressed most often as a one-way crossing incompatibility between infected males and uninfected females and imparts a relative fitness advantage to infected females by decreasing the fitness of uninfected females [11]. Detailed cytological studies in the haplodiploid wasp *Nasonia vitripennis* indicate that a sperm modification in infected males leads to delayed nuclear envelope breakdown of the male pronucleus [12] and resultant, improper condensation of the paternal chromosomes after fertilization of the uninfected egg [13]. Abnormal embryonic development of the egg ensues and the paternal chromosomes are ultimately lost. Maternal chromosomes segregate properly, resulting in haploid male progeny in *N. vitripennis* [14] but embryonic death in diploid insects like *Drosophila* [15]. When the fertilized egg is infected with the same *Wolbachia* strain as that in the male, fertilization and embryonic development occurs normally. There is considerable interest in the role of CI as a biocontrol tool to curb the spread of arthropod-borne pathogens and agricultural pests [16,17] as well as a rapid speciation mechanism in insects [10].

CI can be partial or complete, in which some or no progeny are produced in incompatible crosses between infected males and uninfected females, respectively [11]. Despite the efforts devoted to characterizing CI since the 1950′s, the microbial

Editor: David Schneider, Stanford University, United States of America

Received December 9, 2005; **Accepted** April 5, 2006; **Published** May 19, 2006

DOI: 10.1371/journal.ppat.0020043

Abbreviations: CI, cytoplasmic incompatibility; RT-qPCR, real-time quantitative polymerase chain reaction; TEM, transmission electron microscopy

* To whom correspondence should be addressed. E-mail: sbordenstein@mbl.edu

¤ Current address: University of Connecticut, Storrs, Connecticut, United States of America

Synopsis

Symbiotic bacteria that are maternally inherited are widespread in terrestrial invertebrates. Such bacteria infect the cells of reproductive tissues and can have important evolutionary and developmental effects on the host. Often these inherited symbionts develop beneficial relationships with their hosts, but some species can also selfishly alter invertebrate reproduction to increase the numbers of infected females (the transmitting sex of the bacteria) in the population. Bacterial-mediated distortions such as male-killing, feminization, parthenogenesis induction, and cytoplasmic incompatibility are collectively known as "reproductive parasitism." In this article, the investigators show that the associations between the most common reproductive parasite in the biosphere *(Wolbachia)* and a parasitic wasp host are affected by a mobile element—a temperate bacteriophage of *Wolbachia*. In contrast to recent reports that suggest bacteriophage WO-B may induce reproductive parasitism, the authors' quantitative and ultrastructural analyses indicate that lytic phage WO-B are lethal and therefore associate with a reduction in both *Wolbachia* densities and reproductive parasitism. Based on these data, the authors propose a phage density model in which lytic phage development specifically leads to a reduction, rather than induction, of reproductive parisitism. The study is among the first investigations to show that lytic bacteriophage inversely associate with the densities and phenotype of an obligate intracellular bacterium.

factors that shape CI variation have remained mostly elusive with the exception that *Wolbachia* densities positively associate with incompatibility levels within strains. This observation is known as the "bacterial density" model of CI [18] and numerous studies have confirmed the pattern with correlates between CI levels and counts of bacterial densities in infected eggs, infected sperm cysts, or whole adults [19–22]. Because *Wolbachia* are not present in sperm from infected males, the modification [23] leading to partial or complete CI must take place before the completion of spermatogenesis in infected testes [24–26]. Extrinsic factors that modulate incompatibility strength and type have been more readily detected and include host genetic background [27–29] and environmental stresses such as host age [15,30], heat treatment [31], mating history [32], and larval crowding [33] that can reduce bacterial densities. No studies have yet determined the effect of microbial factors, such as bacteriophage, on bacterial density variation and the expression of CI. Furthermore, the general function of bacteriophages in maternally transmitted symbionts is paradoxical itself since these bacteria tend to have a confined intracellular niche and an accelerated rate of mobile element loss [34–36].

Wolbachia, Candidatus *Hamiltonella defensa*, and *Spiroplasma* are the only known maternally transmitted arthropod endosymbionts with bacteriophage elements [37–39]. The full genome sequence of *Wolbachia w*Mel revealed three prophage regions: a small pyocin-like element, *w*Mel WO-A, and *w*Mel WO-B [40]. Recently, bacteriophage WO-B of *Wolbachia* has received heightened interest in regards to its ability to form mature virion particles [41,42], horizontally transfer between coinfecting strains [43,44], and serve as a molecular marker for *Wolbachia* strain typing [45]. Ankyrin repeats—a common protein sequence motif that mediate interactions between a wide spectrum of proteins including cytoskeletal organizers and cell cycle regulators—are embedded in genes of prophage WO-A and WO-B that are predicted to be highly expressed [40]. Notably, CI appears to result from changes in cell cycle regulatory proteins [46] that might be mediated by genes containing such ankyrin repeats. In addition, the 20.5-kb WO-B virion genome also carries a gene with putative virulence function *(VrlC)* that may encode effector proteins associated with the phage or type IV secretion system of *Wolbachia* [42]. Sex-specific expression of two phage-associated genes has also been observed [29,47]. For these reasons, bacteriophage WO-B has been tentatively proposed as a genetic candidate for inducing CI [29,42,48], but there is inconsistent evidence on whether WO-B sequence diversity correlates with CI crossing type [49,50]. It remains unclear whether bacteriophage actually encode genes directly involved in CI, and whether the temperate WO-B can influence *Wolbachia* during its lytic or lysogenic development. We suggest that clarifying the separate roles of lytic and lysogenic phage development in *Wolbachia* biology will effectively structure inquiries into this research topic.

Here we consider the role of lytic development in association with *Wolbachia* densities and penetrance of reproductive parasitism. We propose a "phage density" model in which lytic development of temperate bacteriophage WO-B, encompassing processes such as DNA replication, virion formation, and cell lysis, leads to the reduction rather than induction of CI (Figure 1). Our rational is that lysis or negative physiological effects of replicating phage on *Wolbachia* cell cycle processes could reduce or maintain low bacterial densities. Since *Wolbachia* densities positively associate with incompatibility levels in many systems [19–22], phage replication could lead to a reduction in CI. This hypothesis is simple and clarifies the role that lytic phage may have on the biology of *Wolbachia,* but does not rule out a role for lysogenic phage in the expression of CI. Revealing the microbial genetic factors that modulate CI will significantly enhance our understanding of how *Wolbachia* endosymbionts override normal host reproductive strategies. In addition, the studies described here comprise the first investigation of how bacteriophage lifecycle generally associates with the density and phenotype of an obligate intracellular bacterium.

Results/Discussion

We report a set of interconnected experiments that highlight the density and ultrastructure relationships between bacteriophage WO-B, *Wolbachia,* and by association, reproductive parasitism. By enumerating CI levels and microbial abundances from individual A- and B-infected *N. vitripennis* males, we characterize variation in CI strength and

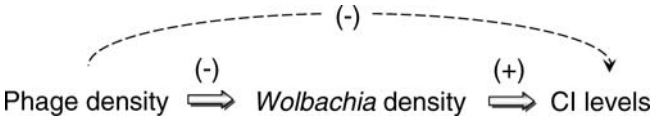

Figure 1. A Phage Density Model of CI

This flowchart depicts the predicted associations, i.e., (–) negative and (+) positive, between phage densities, *Wolbachia* densities, and CI levels with arrows connecting the associated variables. The flowchart is based on the following hypothesis: if lytic development of temperate phage WO-B leads to bacterial lysis or slowed cell divisions, the relative copy number of phages per bacterium may negatively associate with the relative copy number of *Wolbachia* per host, which in turn is well established to positively associate with CI levels. Under this scenario, phage densities can have a secondary negative association with CI levels.
DOI: 10.1371/journal.ppat.0020043.g001

phage and bacterial densities, and analyze the correlates between these three variables. Ultrastructural analyses are conducted to validate the quantitative PCR findings and revealed a moderate frequency of virion-containing *Wolbachia* in an often degenerate and lysed state, as well as putative aggregations of extracellular virions. Observed interactions between *Wolbachia* membrane and individualized spermatids are also reported.

CI in *N. vitripennis*

In the haplodiploid *N. vitripennis,* compatibility is measured by the number of diploid females produced among progeny because only diploid females result from fertilization. Since normal compatible sex ratios under the experimental design are female biased (80% to 95%), incompatibility is expressed as a reduction in the number of female progeny.

To measure *Wolbachia*-induced CI, we first crossed single infected males of *N. vitripennis* harboring one of the two main strains of arthropod *Wolbachia* (A or B) to single uninfected females and scored F1 progeny numbers and sex ratios from these incompatible crosses (Table 1). Control crosses with uninfected males and females were run concurrently for comparison. Crosses with A-infected and B-infected males elicit significantly different patterns of CI. B-infected males induce complete incompatibility as evident by a 100% reduction in the number of diploid females in comparison to that of the uninfected (U) control crosses (Mann-Whitney *U*, $p < 0.0001$), while A-infected males induce significant, partial incompatibility (67% reduction) in comparison to uninfecteds (Mann-Whitney *U*, $p < 0.0001$) (Figure 2). Because *N. vitripennis* harbor putative nuclear genes that convert fertilized eggs from CI crosses into haploid eggs carrying only the maternal chromosomes [51], there is also a corresponding increase in the number of haploid males in both sets of incompatible crosses compared to that of the control crosses (Mann-Whitney *U*, $p < 0.0001$). Effects of host genetic background on the CI level differences observed between A and B *Wolbachia* are mitigated by the derivation of these stocks from the same doubly-infected strain [52] and the consistency of our CI penetrance data with previous findings using these same *N. vitripennis* stocks [51,52].

Relationship of Phage WO-B and *Wolbachia* Copy Number

To examine *in vivo* copy numbers of bacteriophage and *Wolbachia* from the infected males above, we used real-time quantitative polymerase chain reaction (RT-qPCR) and enumerated single copy genes of the *N. vitripennis* genome (S6 kinase or *S6K*), *Wolbachia* genome *(groEL),* and phage WO-B genome (ORF7) (Table 1). These gene copy counts then reflect total microbial abundances in *N. vitripennis* males. The plaque assay is the traditional method for the quantification of bacteriophages, but is not applicable to unculturable endosymbionts. RT-qPCR is instead a more precise and reliable alternative to the plaque assay [53] and allows simultaneous quantification of different gene copy numbers using a common methodology.

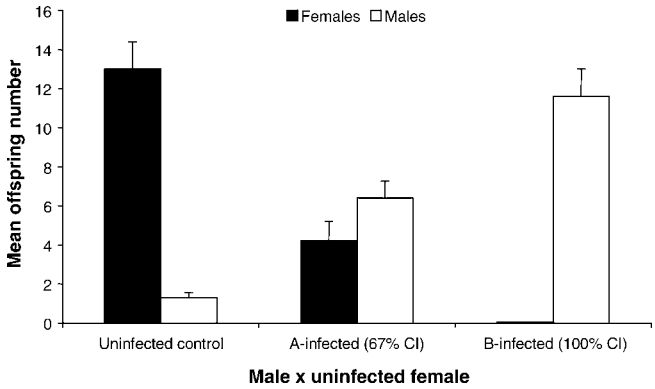

Figure 2. *Wolbachia*-Induced CI in *N. vitripennis*

Mean offspring number ± SE are shown for crosses between uninfected females and single males that are uninfected ($n = 15$), A-infected ($n = 20$), or B-infected ($n = 24$). % CI is calculated as 100% − (mean number of females in an incompatible cross/mean number of females in the control compatible cross) × 100.

DOI: 10.1371/journal.ppat.0020043.g002

Figure 3 shows that total bacteriophage WO-B abundance is strongly correlated with total bacterial abundance for both A *Wolbachia* (rho = 0.9814, $p < 0.0001$) and B *Wolbachia* (rho = 0.9537, $p < 0.0001$), as expected for a temperate bacteriophage in which a lysogenic phage is cotransmitted with the bacterial host and lytic infection depends on the bacterial encounter frequency. However, the total phage and bacterial gene copy numbers are strikingly far greater for A *Wolbachia* than B *Wolbachia* (Table 1). The bacteriophage ORF7 and *Wolbachia groEL* copy number means for A-infected males are at least an order of magnitude greater than that of B-infected males, respectively (Mann-Whitney *U*, $p < 0.0001$ for both comparisons). The larger genomic abundances of A versus B *Wolbachia* and their associated phage are noteworthy given that A *Wolbachia*–infected males express incomplete CI while B *Wolbachia*–infected males express complete CI. A *Wolbachia*

Table 1. Summary Statistics from Quantitative PCR and CI Experiments Using A and B *Wolbachia*

Male Strain	*N*	Mean Copy Number ($\times 10^5$) ± SE			Mean Density ± SE		CI		
		Insect S6 Kinase	*Wolbachia groEL*	Phage WO-B ORF7	*Wolbachia* (*groEL*:S6K)	Phage WO-B (ORF7:*groEL*)	Number of Males	Number of Females	Percent CI
N. vitripennis U	15	—	—	—	—	—	1.3 ± 0.3	13.0 ± 1.4	0.0
N. vitripennis A	20	37.1 ± 1.6	2.7 ± 0.4	14.6 ± 1.7	0.08 ± 0.01	5.8 ± 0.29	6.4 ± 0.9	4.2 ± 1.0	67.7
N. vitripennis B	24	36.5 ± 1.1	0.2 ± 0.02	0.3 ± 0.03	0.01 ± 0.00	1.6 ± 0.12	11.6 ± 1.4	0.0 ± 0.0	100

Single infected (A and B) and control uninfected (U) *N. vitripennis* males were crossed to uninfected females to determine percent CI, and their DNA was subsequently used for enumerating insect, *Wolbachia,* and bacteriophage gene copy numbers. Percent CI in the haplodiploid *N. vitripennis* is calculated as 100% − (the mean number of females in an incompatible cross/mean number of females in compatible control cross) × 100.

SE, standard error.

DOI: 10.1371/journal.ppat.0020043.t001

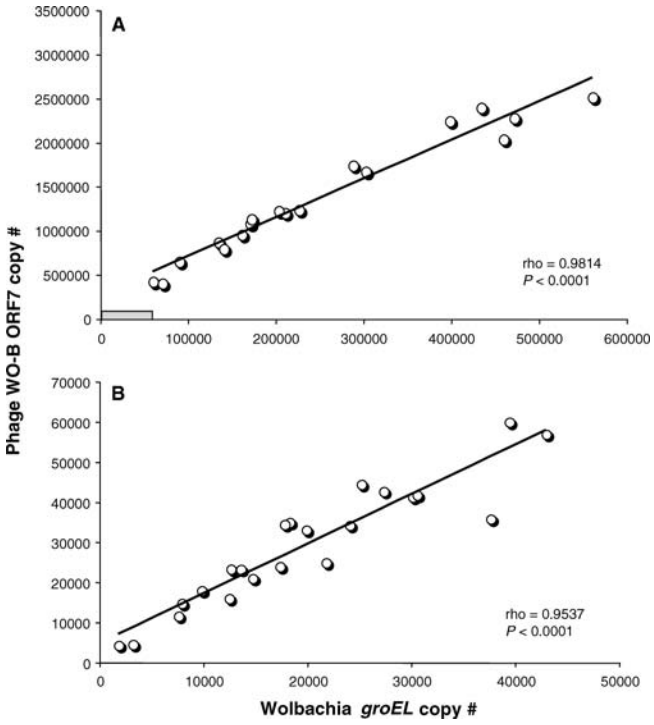

Figure 3. The Associations of Temperate Phage WO-B and *Wolbachia* Abundance

Points on the charts denote the absolute copy numbers of a single-copy gene for phage WO-B and *Wolbachia* in individual adults of (A) A-infected males and (B) B-infected males of *N. vitripennis*. Correlation coefficients and significances are calculated according to the non-parametric method of Spearman's rho. In (A), the gray rectangle denotes the relative range of copy number variation for B-infected males, as depicted in larger scale in (B).

DOI: 10.1371/journal.ppat.0020043.g003

apparently have a higher density threshold for inducing complete CI than B *Wolbachia* in *N. vitripennis* males. These total abundance differences are not due to host body size differences between the A- and B-infected males (Insect S6K counts, Mann-Whitney *U*, $p = 0.8137$) and indicate, as other studies have, that abundance data among divergent *Wolbachia* strains are not comparable in relation to CI level variability [54,55].

Associations between Phage, Bacteria, and CI Penetrance

We tested the three associations predicted by a phage density model (Figure 1). We used data strictly from the A *Wolbachia*–infected males as they show variability in the strength of incompatibility. A-infected males inducing nearly complete CI (specified as none to one F1 female) have an average *Wolbachia* density (*groEL* copy number/*S6K* copy number) of 0.114, while B-infected males which all induce complete CI have an average density of 0.01 ($p < 0.0001$, Mann-Whitney *U*). Furthermore, A-infected males inducing partial CI (specified as two F1 females or more) have a significantly lower average density (0.048) than similarly infected males expressing complete CI ($p = 0.0036$, Mann-Whitney *U*). The results are again consistent with the bacterial density model and an inability to compare density relationships of the divergent A and B *Wolbachia*.

Calculations of phage copies per *Wolbachia* copies support the temperate lifestyle of WO-B in *N. vitripennis* A *Wolbachia*. We previously identified four different ORF7 paralogs in the *N. vitripennis* A *Wolbachia* through cloning and sequencing of heterogeneous PCR products [44]. Thus, at a minimum, we expect a ratio of four phage genes per bacterium during lysogeny. Our RT-qPCR data confirm this estimate, as the phage-to-bacteria ratio exceeds 4 in all cases (Figure 4A). The phage WO-B density (ORF7 copy number/*groEL* copy number) ranges from 4.44 to 7.31 with an average of 5.83. We also previously identified one ORF7 homolog in the B *Wolbachia* and the enumerated phage-to-bacteria ratio exceeds 1 in all cases (unpublished data) with an average of 1.6 (Table 1). Genomic copy number per cell in *Wolbachia* of *Brugia malayi* was estimated to be one [56]. If this holds in the A *Wolbachia* of *N. vitripennis,* then our results may be interpreted as an average ratio of 5.83 phages per bacterium. The consistency between the sequence data and quantitative PCR data suggests that phage WO-B may encode repressors that prevent lysogeny of genetically identical or similar phage. Such repression is typical of other temperate bacteriophages. The overall variation in phage densities suggests that phage are replicating and undergoing lytic development at a moderate rate. Quantitative electron microscopy data support this inference (see below).

The phage density model in Figure 1 directly predicts that phage densities will inversely associate with *Wolbachia* densities based on the basic tenets that (i) bacteriophages are predators of bacteria and (ii) lytic development will inhibit bacterial replication or induce cell lysis. Microscopic observations of virion-containing *Wolbachia* exhibit cell lysis [41] or intracellular pyknotic-like patches indicative of cell death [37]. Consistent with these observations, we report a strong and significant inverse association between phage and A *Wolbachia* densities in *N. vitripennis* males (rho = –0.7525, $p = 0.0005$, Figure 4A). For instance, the highest WO-B densities (up to 7.31 per *Wolbachia* genome) have the lowest *Wolbachia* densities (Figure 4A) and lowest absolute abundance of *Wolbachia* (less than 1×10^5 *groEL* copies) for the entire dataset and vice versa. These findings specify that samples with the highest densities of lytic phage WO-B associate with *Wolbachia* experiencing the slowest rates of replication or a phage-mediated reduction in *Wolbachia* densities.

The RT-qPCR data also validate the bacterial density model: a direct, positive relationship between *Wolbachia* densities and CI strength (Figure 4B). Since CI in haplodiploids is measured as a reduction in the number of diploid females produced, we present the analysis as number of surviving, female offspring produced from incompatible crosses plotted against microbial densities. As a result, the predicted trend is that low numbers of female offspring, i.e., high CI inducers, will associate with high *Wolbachia* densities. As predicted, we found that female offspring numbers and *Wolbachia* densities in infected males showed a significant negative association (rho = –0.6352, $p = 0.0046$). The higher numbers of female offspring per male (more compatibility) associate with the lower *Wolbachia* densities, while the lower numbers of female offspring per male (more incompatibility) associate with the higher *Wolbachia* densities. The data therefore corroborate the bacterial density model in infected *N. vitripennis* males, in comparison to previous techniques that scored bacterial densities in eggs [18].

From the negative association between phage WO-B and *Wolbachia* densities, and the positive association between *Wolbachia* densities and CI levels, it follows that phage WO-B densities could indirectly associate with CI penetrance by

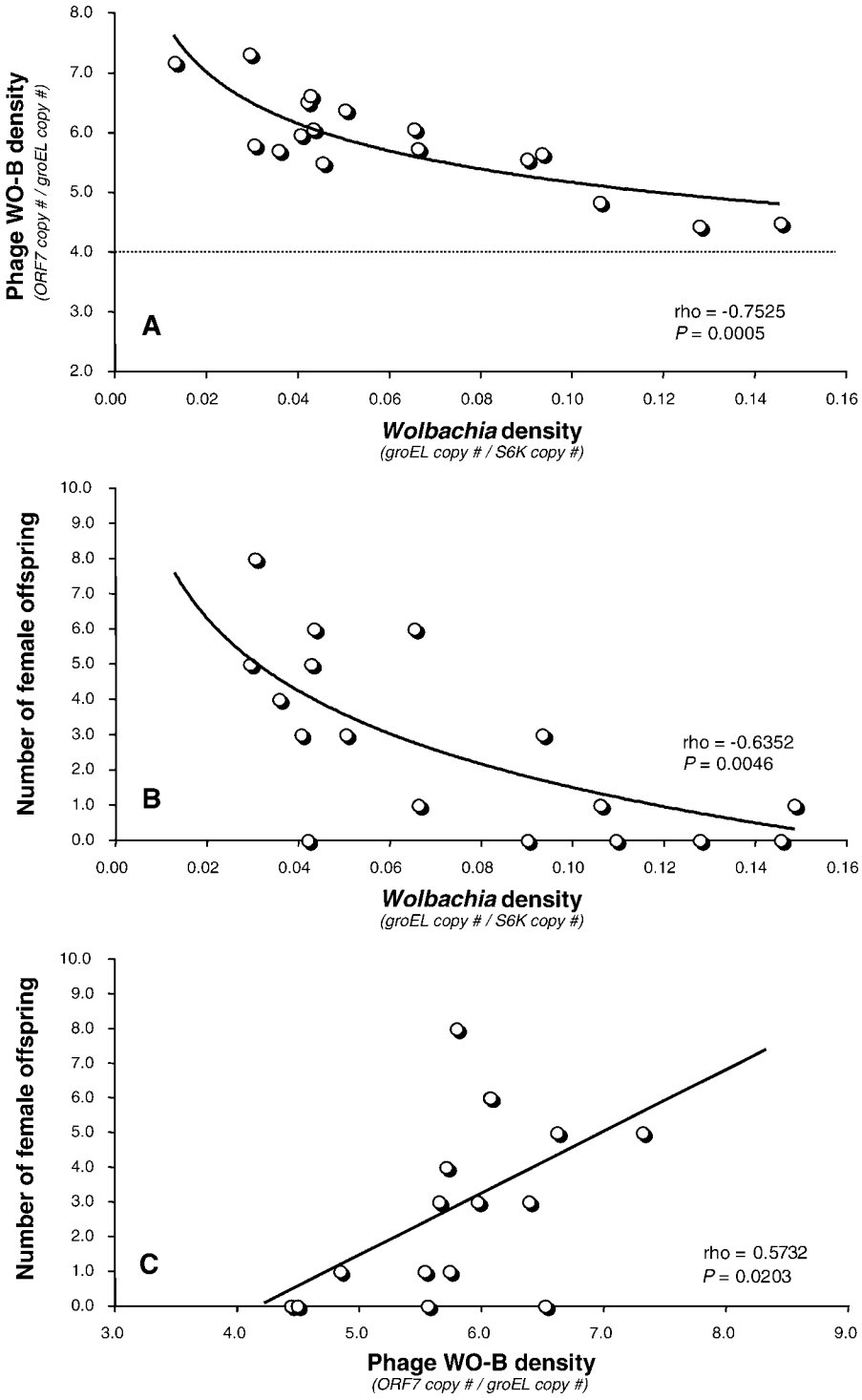

Figure 4. The Relationships between Phage Density, *Wolbachia* Density, and CI Level

Points on the charts denote the relative phage WO-B density, relative *Wolbachia* density, and the number of female (diploid) offspring produced from cytoplasmically incompatible crosses using A-infected males. CI in haplodiploid species is expressed as a reduced number of female offspring. In (A), the dashed line denotes the estimated number of different lysogenic WO-B prophages per A-*Wolbachia* genome as determined by OFR7 amplification, cloning, and sequencing of heterogeneous copies [44].

DOI: 10.1371/journal.ppat.0020043.g004

virtue of a second-order correlation (Figure 1). The basic reason is that phage-mediated cell lysis will simultaneously decrease *Wolbachia* densities and increase phage densities, as evident in Figure 4A. Percentages of lytic *Wolbachia* per male are the ideal data point to correlate to CI levels, but are difficult to assess in practice owing to the unculturability of *Wolbachia*. Enumerated phage densities are thus a proxy for lytic development since increasing phage densities results from lytic development. Caveats to using this proxy include (i) variation in phage densities could be accounted for by

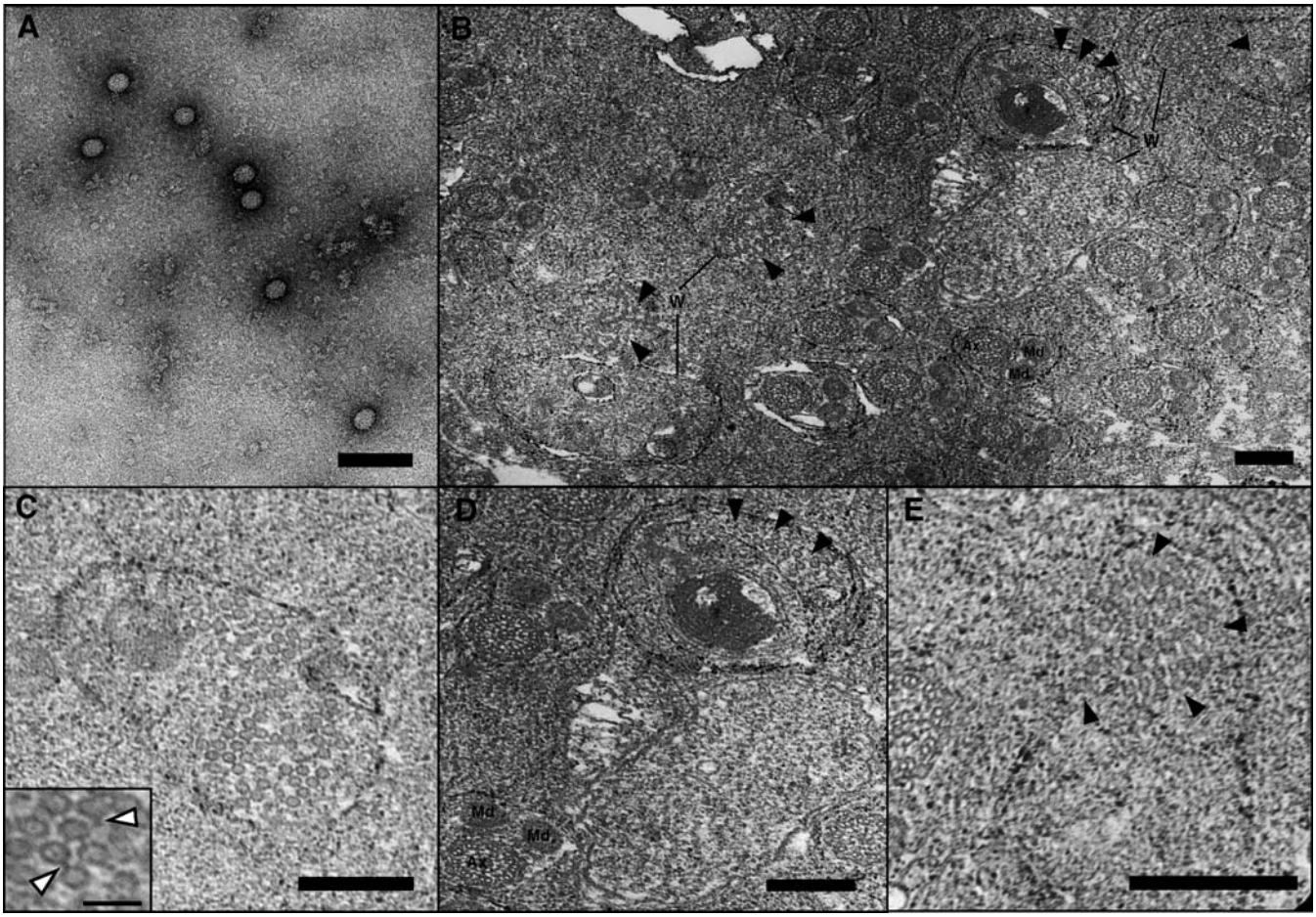

Figure 5. *Wolbachia* Infecting the Testes of *N. vitripennis*

(A) Negatively stained virus particles of uniform size from PEG-precipitated preparations of A-infected *N. vitripennis* adults. No tail-like structures were apparent, perhaps due to disruption during the purification process. Bar = 100 nm.

(B) Low-resolution transmission electron micrograph of individualized spermatids and *Wolbachia* in *N. vitripennis* pupal testes. Ax and Md denote spermatid axonemes and mitochondrial derivatives. Several of the noted *Wolbachia* cells (W) are shown in higher resolution in Figure 5C–5E. Solid arrowheads denote phage particles. Bar = 200 nm.

(C) A high density of phage particles within *Wolbachia* is shown; phage tails are occasionally visible and noted by white arrowheads in the inset. Bar = 200 nm; inset bar = 100 nm.

(D) Virion-free (lower right) and virion-containing *Wolbachia* (upper right) localized near two *N. vitripennis* spermatids are shown. Solid arrowheads denote phage particles inside *Wolbachia,* and Ax and Md denote spermatid axonemes and mitochondrial derivatives, respectively. Bar = 200 nm.

(E) Solid arrowheads denote phage particles dispersing from within putatively lysed *Wolbachia* into the extracellular matrix. Bar = 200 nm.

DOI: 10.1371/journal.ppat.0020043.g005

variability in the number of virions produced per bacteria. However, if the variation was strictly due to variable numbers of virions produced by the same number of *Wolbachia* in infected males, then we would not observe the corresponding variation in A *Wolbachia* abundances evident from the correlate in Figure 3A and (ii) *Wolbachia* densities do not perfectly correlate with phage densities or CI penetrance as evident by the coefficient values of rho = −0.7525 (Figure 4A) and rho = −0.6352 (Figure 4B), respectively. The variation not accounted for in these correlation coefficients will further amplify the noise in the indirect, second-order correlation analysis between phage densities and CI levels.

Despite the caveats, Spearman's rho correlation analysis reveals a positive and tentatively significant relationship between phage WO-B densities and female offspring numbers following the removal of four outliers identified by the jackknifed Mahalanobis Distance (rho = 0.5732, $p = 0.0203$, Figure 4C). The higher numbers of female offspring per male (more compatibility) associate with the higher phage WO-B densities (more lytic development), while the lower numbers of female offspring per male (more incompatibility) associate with the lower phage WO-B densities (less lytic development). The data thus tentatively corroborate the phage density model in infected *N. vitripennis* males. As a further analysis of the data, we performed two nonparametric pairwise comparisons to test the hypothesis that males expressing nearly complete CI (none to one F1 female) have lower phage densities than males expressing incomplete CI (two F1 females or more). The Mann-Whitney U tests are significant both before ($p = 0.0261$) and after ($p = 0.0064$) the removal of the four outliers identified above.

In total, the combination of support for all three associations is consistent with an inverse relationship between lytic phage and *Wolbachia* densities and reproductive parasitism. Based on these tripartite associations, we suggest that lytic phage indirectly repress CI by negatively affecting *Wolbachia* fitness through cell lysis and/or slowed replication rates. However, we caution that this correlative evidence does

Table 2. Summary of TEM in Late Pupal Testes

Criterion	Value
Testes regions examined from two males	12
Total micrographs	25
Range of magnifications	×5,450 to ×54,400
Total *Wolbachia* observed	51
Virion-containing *Wolbachia*	6
Mean number of virions per *Wolbachia*	24.7
Range of virions per *Wolbachia*	4–65
Wolbachia in putative contact with spermatids	8
Putative patches of extracellular virions	11

DOI: 10.1371/journal.ppat.0020043.t002

not prove causation and the role of lysogenic phage (i.e., prophage gene expression) in reproductive parasitism awaits a full transcriptome characterization.

Confirmation of Lytic Development of Bacteriophage WO-B

We employed transmission electron microscopy (TEM) to directly confirm the lytic phage development evident from the quantitative PCR studies. Figure 5A shows an electron micrograph of negatively stained virion particles collected from whole A-infected *Nasonia* homogenizations and serial filtrations through 0.45-μm and 0.22-μm filters. Genomic isolation of these filtrated virions and PCR assays indicated that the filtrate contains phage WO-B, and is free of *Wolbachia* contamination. The virion sizes are the same as those observed inside *Wolbachia* from micrographs of random thin sections of infected, pupal testes (Figure 5B–5E). These thin section micrographs revealed a range of virion-containing ($n = 6$) and virion-free *Wolbachia* ($n = 45$). *Wolbachia* bacteria ranged in size from 300 nm to 1 μm in length and 250 to 590 nm in width, with usually three observable membranes consisting of the host vacuole, the cell wall, and plasma membrane. Spermatogenesis is synchronized in *N. vitripennis* and mostly complete during the late pupal stages [57]. As a result, *Wolbachia* were closely associated with the sperm flagellar axoneme and mitochondrial derivatives of individualized spermatids (Figure 5B), which is consistent with other insects [58,59]. Based on the observed proportion of virion-containing *Wolbachia* in infected testes (Table 2, Figure 5B–5E), 11.76% of *Wolbachia* cells were determined to be experiencing lytic phage development. This percentage is approximately less than half of that observed in micrographs of ovary-infecting *Wolbachia* in *Culex pipiens* [37]. The mean number of virions per infected *Wolbachia* in our observations was 24.7. Based on these estimates and sequence data indicating four lysogenic phages per *Wolbachia* [44], we can back-calculate a tentative estimate of the TEM-observed ratio of phage copies per *Wolbachia* using the following equation: [(the average number of observed virions per *Wolbachia* plus an estimated four lysogenic phages per *Wolbachia*) × (observed frequency of virion-containing *Wolbachia*)] + [(four lysogenic phages per *Wolbachia*) × (the observed frequency of virion-free *Wolbachia*)]. This equation [(24.66 + 4.0)(0.1176)] + [(4.0)(0.8829)] yields an estimate of 6.9 phage copies per *Wolbachia*, a number that parallels the real-time quantitative PCR estimate of an average density of 5.8 phages per bacterium. Despite many assumptions requiring proper caution, it can be concluded that the consistency of the RT-qPCR and TEM studies, and relatively low frequency of observed virion-containing *Wolbachia* (11.78%), produces an overall, moderate intrahost ratio of phage to bacteria.

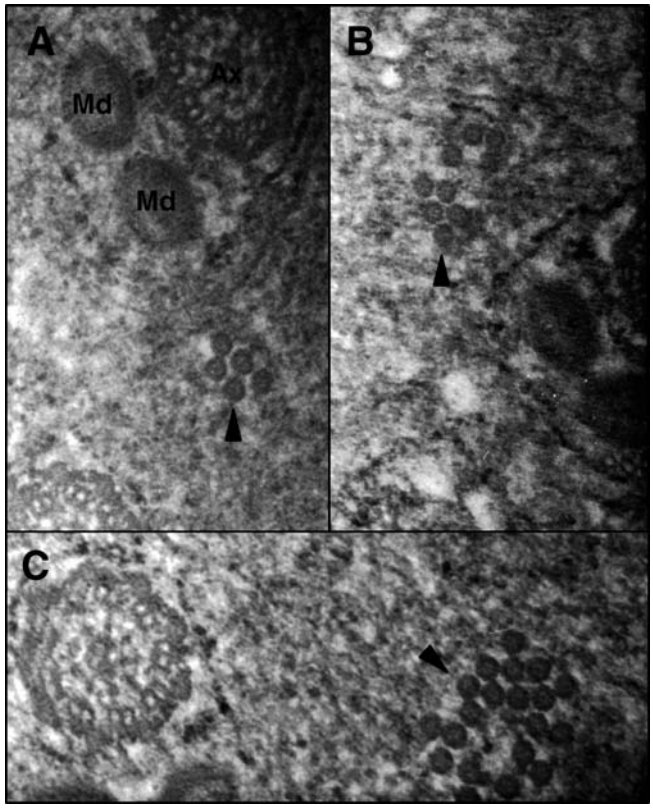

Figure 6. Aggregations of Putative Extracellular Virions

Solid arrowheads denote phage particles with no detectable *Wolbachia* membrane surrounding them. In some cases, a single membrane structure can be seen either completely or partially surrounding the phage particle patches.

(A) A patch of five virions near an individualized spermatid, for size reference.

(B) A patch of nine virions to the left of an individualized spermatid.

(C) A patch of 20 virions near a flagellar axoneme with potentially a single membrane structure surrounding the patch.

DOI: 10.1371/journal.ppat.0020043.g006

The icosehedral virions of *Wolbachia* ranged in diameter from 35 to 45 nm, some of which had an observable tail-like structure that ranged in length from 10 to 20 nm. Bacteriophage tails are typically required for host membrane attachment and infection. Particles were distributed along the inner membrane and in the middle of the cell, which was often irregularly shaped, degenerative, and lysed. We observed virion-containing *Wolbachia* with dense masses in the middle of the cell and detached membrane structures analogous to phage-infected *Chlamydia* [60] (Figure 5D). The range of virions per *Wolbachia* widely varied from four to 65. In at least three of six cases, virions were observed leaving lysed cells into the extracellular matrix (Figure 5E), indicating the phage particles are lethal to *Wolbachia*. Aggregations of similarly sized viral particles were also observed in the extracellular matrix of the testes (Figure 6A–6C). No detectable *Wolbachia* occurred around these patches, indicating that these virion clusters probably departed from the bacterial cell. Single membrane structures completely or partially surrounding the patches may be present, but can not be confirmed based on the micrographs.

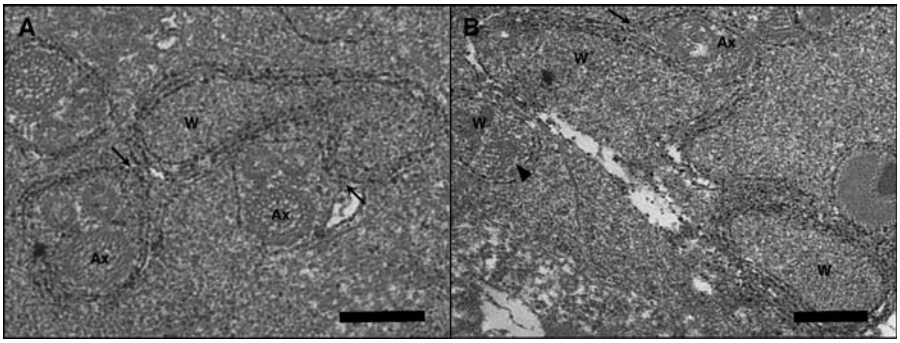

Figure 7. *Wolbachia* Membrane Associates with Spermatid Tails in the Testes of *N. vitripennis*

Arrows indicate regions of contact between virion-free *Wolbachia* and spermatids. Ax denotes flagellar axonemes. W denotes *Wolbachia*.
(A) Contact between a single *Wolbachia* cell and two individual spermatids. Bar = 200 nm.
(B) The membrane of a dividing *Wolbachia* (upper left) associates with a putative spermatid along the junction indicated by arrow. Ax denotes axonemal structure. Solid arrowhead denotes virion particles within neighboring *Wolbachia* (middle left). Bar = 200 nm.
DOI: 10.1371/journal.ppat.0020043.g007

Interactions between *Wolbachia* Cells and Spermatids

It has been hypothesized that the mechanism of CI in crosses between infected males and uninfected females involves an imprinting effect in the testes since mature sperm do not harbor *Wolbachia* [11,23]. Whether sperm imprinting is due to *Wolbachia*-secreted proteins or the uptake of host proteins by *Wolbachia* is currently unresolved, but the discovery of a type IV secretion system in *Wolbachia* has heightened interest in the function of secreted proteins [61]. Our observations with TEM of infected *N. vitripennis* testes unexpectedly revealed cases of *Wolbachia* membrane in contact with or surrounding *N. vitripennis* spermatids (Figure 7). *Wolbachia* are typically spherical or rod-shaped, but *Wolbachia* also appeared twisted in the direction of contact with multiple spermatids (Figure 7A). Only virion-free *Wolbachia* were observed to contact the spermatids. Of the total observed *Wolbachia*, 15.68% were observed in putative contact with membranes of spermatid tails. These observations present the possibility that *Wolbachia* may be responsible for expressing a sperm imprinting effect through direct physical interactions with the developing spermatids, or alternatively in the general tissue matrix of the testes. If the mechanism of CI is dependent or influenced by *Wolbachia*-spermatid contact, then variation in incompatibility strength could be determined by the proportion of spermatids contacted by *Wolbachia*. No direct evidence currently supports this. Recent TEM observations in infected *Drosophila simulans* testes indicated that *Wolbachia* reach their highest densities around elongating spermatids [59]. These observations and mechanistic hypotheses warrant future microscopy studies to determine how common the physical associations are in other incompatibility-inducing *Wolbachia*. Without further investigations, it is not clear what functional relationship, if any, this contact may actually have. We believe these photographs comprise the first documentation of physical contacts between *Wolbachia* and individualized spermatids, probably due to a preference for electron microscopy work in the transmitting sex-infected females.

Summary

Symbiosis impacts all levels of organic complexity. Bacterial endosymbiosis in particular is a hallmark example of the intimate, binary interactions between prokaryotes and eukaryotes. Such interactions are common in animals and have facilitated important insights into the processes affecting cellular complexity, bacterial genome size, and organelle evolution. The surprising discoveries of bacteriophage in some of these endosymbiotic bacteria holds enormous value for further understanding these symbiotic associations and the development of genetic tools in these unculturable systems.

In this study, we examined the tripartite associations and ultrastructure of a phage, bacterial endosymbiont, and host arthropod that collectively represent a widespread and evolutionary important symbiotic system. The effects that lytic phage growth and virion production can have on this tripartite symbiosis span important evolutionary and ecological processes such as lateral phage transfer between *Wolbachia* (virion production is a requisite for mobility and transduction), potential modulation of intracellular *Wolbachia* densities (lytic development may repress bacterial densities), and, by association, penetrance of *Wolbachia*-mediated reproductive parasitism such as CI.

Our quantitative and ultrastructural analyses comprise the first studies to illustrate a negative density relationship between phage WO-B and *Wolbachia*, as expected for an active lytic phage. Ultrastructural analyses confirm the ability of *Wolbachia* phage to form virion particles and lyse the host cell. Furthermore, the negative association between CI levels and phage densities suggests that the genes encoding CI "toxins" apparently are not expressed in replicating or mature phage. Otherwise, we would expect a positive correlation between phage densities and CI levels. Genes in phage WO-B may still encode CI "toxins" while the genome is integrated as a prophage during lysogeny, but a complete transcriptome characterization of the phage during lysogeny is necessary to address this issue. Sex-specific expression of phage-related genes is consistent with a possible role of lysogenic phage in reproductive parasitism and has been observed in infected *Culex* mosquitoes [29,47]. However, an alternative explanation for sex-specific expression is that bacteriophage may have different rates of lytic development in males and females. Selection for increased bacterial transmission efficiency at the bacterial level or suppression of incompatibility levels at the host level may for example promote the evolution of higher lytic development rates and thus expression in infected males. Either of these hypotheses are consistent with a phage density model in which phage are strictly parasitic to *Wolbachia* and do not impart a benefit to the bacterium.

One hypothesis for the widespread distribution of phage WO-B [44] based on this speculation is that the host, rather than *Wolbachia*, benefits from the presence of a lytic phage since host level and phage level selection could both favor an active bacteriophage infection that lyses *Wolbachia* cells and thus reduces the bacterial load in the arthropod host. This host level selection could also explain its absence from mutualistic *Wolbachia* in filarial nematodes [62] in which host level selection would select against a lytic phage of a mutualistic *Wolbachia* that is required for host oogenesis and larval development. The results presented here also raise the interesting possibility that common environmental (e.g., temperature) or host genetic factors known to modulate *Wolbachia* densities do so by inducing prophage excision, virion production, and cell lysis. Future investigations should simultaneously examine the effects of these extrinsic factors on phage and insect endosymbiont densities. Finally, an active and inducible temperate phage in *Wolbachia* is a promising genetic tool to engineer *Wolbachia* for biocontrol strategies or as a biotherapy tool to combat the devastating pathologies of *Wolbachia*-assisted filariasis in humans. It is clear that the *Wolbachia* symbiosis has been shaped by at least three genetic entities and experimental and theoretical studies on their interactions will collectively assemble a general model of the host-reproductive parasite interactions.

Materials and Methods

Insect strains. *N. vitripennis* are gregarious parasitoid wasps of fly pupae. They are raised on *Sarcophaga bullata* (flesh fly) pupae in the laboratory, with constant light and temperature (21 °C). Three strains were used in these studies: a single A-infected strain (12.1), a single B-infected lab strain (4.9), and an uninfected strain (13.2). These strains were derived in 1996 from a double AB-infected isofemale strain by spontaneous loss of *Wolbachia* following prolonged diapause [52].

Tests of CI. All crosses were set up as single pair matings between uninfected virgin females and virgin males of each of the three strains. Only those pairings where copulation occurred within 10 min of observation were used. Males were immediately frozen at −80 °C, and each female was provided with four hosts for feeding and egg laying. After 48 h, the females were transferred to new vials and given a single host for 6 h. Females were then discarded from each vial and the parasitized hosts were left undisturbed until adult emergence in approximately 2 wk. Adults were scored upon death for sex ratios and total family size. Two replicate experiments were performed 8 mo apart.

RT-qPCR. Genomic DNA was isolated using the DNeasy Tissue Kit (Qiagen, Valencia, California, United States) from single adult males and suspended in 70 μl of double-distilled sterile water. Infection status on a subset of these adults was confirmed by PCR with *Wolbachia*-specific primers. RT-qPCR was performed in an iCycler system (Bio-Rad, Hercules, California, United States). Reaction volumes of 25 μl contained 12.5 μl of BioRad SYBR Green Supermix, 10.5 μl of sterile water, 0.5 μl each of 10 μM forward and reverse primer, and 1 μl of target DNA in single wells of a 96-well plate (Bio-Rad). For the selective amplification of a small portion of the *Nasonia S6 Kinase* gene (133 bp), *Wolbachia groEL* (97 bp), and WO-B ORF7 (125 bp), the following primers were designed and employed: NvS6KQTF2 (5′-GGCATTATCTACAGAGATTTG-3′), NvS6KQTR2 (5′-GCTATGACCTTCTGTATCAAG-3′), NvWGroQTF1 (5′-CAACCTTTACTTCCTATTCTTG-3′), NvWGroQTR1 (5′-CTAAAGTGCTTAATGCTTCACCTTC-3′), NvWOF1 (5′-GTCTGGAAAGCTTACAAAAAG-3′), and NvWOR1 (5′-CTCGCCAAAATATAGCCCTGC-3′). PCR conditions comprised an initial melting at 95 °C for 3 min, followed by 40 cycles with melting at 95 °C (15 s) and primer annealing at 55.6 °C (1 min). A melting curve analysis was performed at the end of the PCRs to check for primer-dimers and nonspecific amplification. Standard curves for each gene were constructed with a log10 dilution series of known amounts of PCR products cloned into plasmid vectors using the TOPO TA cloning kit (Invitrogen, Carlsbad, California, United States). RT-qPCR assays were performed in triplicate on all DNAs and two replicate experiments were performed in total.

Statistics. Correlation coefficients were calculated using the non-parametric Spearman's rho methods in JMP version 5.0.1a (SAS Institute Inc., Cary, North Carolina, United States) Multivariate outliers were identified by the jackknifed Mahalanobis Distance in JMP and removed from the datasets (two to four of approximately 24 total data points per dataset). Outliers can artificially increase or decrease the value of a correlation coefficient and their removal can have recommended benefits that are not typically considered in practice [63,64]. Removals of the outliers did not affect the significance of rho for all analyses except that in Figure 4C in which rho = 0.3339 and $p = 0.15$ prior to removal of four outliers. We expect more variability in this correlation analysis since the phage densities and CI strength are only indirectly related. Linear or logarithmic trend lines were added to the charts to illustrate patterns using Microsoft Excel.

Small plate effects are common in RT-qPCR experiments and were apparent by a trend of slightly elevated or reduced threshold cycle (Ct) values for the same template DNA used for the standard curve across two different plates. Before normalization of the plate effects, individual correlation coefficients (Spearman's rho) on the data from each plate were determined to specify the same association trends (positive or negative) by a homogeneity test ([65], Box 15.4) using the z^*-transformation of data for small datasets. Normalization was then performed by reconstructing the RT-qPCR standard curve with the average threshold cycles of the enumerated dilution series across separate plates. Ct values for experimental DNAs for each gene were compared against the "average" standard curve to specify the normalized starting quantities of template DNA. No plate effects were observed after data normalization.

Electron microscopy. Whole-insect homogenates from infected *N. vitripennis* adults (0.5 g) were isolated using buffers and centrifugation steps previously described [42], with the exception that particles were serially filtrated through 0.45-μm filters twice and 0.22-μm filters once. Buffer volumes included 1.73 ml of SM buffer for adult insect homogenizations and 0.2 ml of TM buffer for pellet resuspension. After ultracentrifugation, the viral pellet was resuspended in a final volume of 50 μl of TM buffer. Particles were negatively stained for visualization using a Zeiss 10C A transmission electron microscope (80 kv). For preparation of infected tissue thin sections, testes of late pupal stage males were dissected in 1× PBS + 0.1% Tween. Tissue was immediately fixed in 2% glutaraldehyde in 0.2M phosphate buffer (pH 7.4) for 2 h at room temperature, washed in 1× PBS three times, and postfixed with 1% osmium tetroxide in buffer for 1 h on ice. Following three 10-min washes in buffer, tissue was dehydrated in graded ethanol series (50% to 100%) and propylene oxide and then embedded in Epon/Araldite resin. Random thin sections of approximately 70 nm were cut using a diamond knife and ultramicrotome (Reichert-Jung), mounted on grids, and stained with 2% uranyl acetate and Reynolds lead citrate for 20 and 15 min, respectively.

Acknowledgments

The authors thank Dr. Sibel I. Karchner for helpful advice on RT-qPCR and Louis Kerr for help with TEM.

Author contributions. SRB and JJW conceived and designed the experiments. SRB, MLM, AJF, UK, and JJW performed the experiments. SRB, MLM, and AJF analyzed the data. SRB and JJW contributed reagents/materials/analysis tools. SRB, MLM, and JJW wrote the paper.

Funding. This work was supported by grants from the NASA Astrobiology Institute (NNA04CC04A) and National Institutes of Health (R01 GM62626-01) to JJW, and by the Marine Biological Laboratory's Program in Global Infectious Diseases, funded by the Ellison Medical Foundation, to SRB. This work was in part performed while SRB held a National Research Council Research Associates Award at the Marine Biological Laboratory.

Competing interests. The authors have declared that no competing interests exist. ■

References

1. Stouthamer R, Breeuwer JA, Hurst GD (1999) *Wolbachia pipientis*: Microbial manipulator of arthropod reproduction. Annu Rev Microbiol 53: 71–102.
2. Breeuwer JA, Jacobs G (1996) *Wolbachia*: Intracellular manipulators of mite reproduction. Exp Appl Acarol 20: 421–434.
3. Jeyaprakash A, Hoy MA (2000) Long PCR improves *Wolbachia* DNA amplification: wsp sequences found in 76% of sixty-three arthropod species. Insect Mol Biol 9: 393–405.
4. Werren JH, Windsor DM (2000) *Wolbachia* infection frequencies in insects: Evidence of a global equilibrium? Proc R Soc Lond B Biol Sci 267: 1277–1285.
5. Jiggins FM, Hurst GD, Majerus ME (2000) Sex-ratio-distorting *Wolbachia*

causes sex-role reversal in its butterfly host. Proc R Soc Lond B Biol Sci 267: 69–73.
6. Rigaud T, Juchault P, Mocquard JP (1997) The evolution of sex determination in isopod crustaceans. Bioessays 19: 409–416.
7. O'Neill SL, Karr TL (1990) Bidirectional incompatibility between conspecific populations of *Drosophila simulans*. *Nature* 348: 178–180.
8. Shoemaker DD, Katju V, Jaenike J (1999) *Wolbachia* and the evolution of reproductive isolation between *Drosophila recens* and *Drosophila subquinaria*. Evolution 53: 1157–1164.
9. Bordenstein SR, O'Hara FP, Werren JH (2001) *Wolbachia*-induced incompatibility precedes other hybrid incompatibilities in *Nasonia*. Nature 409: 707–710.
10. Bordenstein SR (2003) Symbiosis and the origin of species. In: Bourtzis K, Miller TM, editors. Insect symbiosis. New York: CRC Press. pp. 283–304.
11. Bourtzis K, Braig HR, Karr TL (2003) Cytoplasmic incompatibility. In: Bourtzis K, Miller TM, editors. Insect symbiosis. New York: CRC Press. pp. 217–246.
12. Tram U, Sullivan W (2002) Role of delayed nuclear envelope breakdown and mitosis in *Wolbachia*-induced cytoplasmic incompatibility. Science 296: 1124–1126.
13. Reed KM, Werren JH (1995) Induction of paternal genome loss by the paternal-sex-ratio chromosome and cytoplasmic incompatibility bacteria (*Wolbachia*): A comparative-study of early embryonic events. Mol Reprod Dev 40: 408–418.
14. Breeuwer JA, Werren JH (1990) Microorganisms associated with chromosome destruction and reproductive isolation between two insect species. Nature 346: 558–560.
15. Hoffmann AA, Turelli M, Simmons GM (1986) Unidirectional incompatibility between populations of *Drosophila simulans*. Evolution 40: 692–701.
16. Sinkins SP, Curtis CF, O'Neill SL (1997) The potential application of inherited symbiont systems to pest control. In: O'Neill SL, Hoffmann AA, Werren JH, editors. Influential passengers. New York: Oxford University Press. pp. 153–175.
17. Aksoy S, Rio RVM (2005) Interactions among multiple genomes: Tsetse, its symbionts and trypanosomes. Insect Biochem Mol Biol 35: 691–698.
18. Breeuwer JAJ, Werren JH (1993) Cytoplasmic incompatibility and bacterial density in *Nasonia vitripennis*. Genetics 135: 565–574.
19. Poinsot D, Bourtzis K, Markakis G, Savakis C, Mercot H (1998) *Wolbachia* transfer from *Drosophila melanogaster* into *D. simulans*: Host effect and cytoplasmic incompatibility relationships. Genetics 150: 227–237.
20. Perrot-Minnot MJ, Werren JH (1999) *Wolbachia* infection and incompatibility dynamics in experimental selection lines. J Evol Biol 12: 272–282.
21. Noda H, Koizumi Y, Zhang Q, Deng K (2001) Infection density of *Wolbachia* and incompatibility level in two planthopper species, *Laodelphax striatellus* and *Sogatella furcifera*. Insect Biochem Mol Biol 31: 727–737.
22. Veneti Z, Clark ME, Zabalou S, Karr TL, Savakis C, et al. (2003) Cytoplasmic incompatibility and sperm cyst infection in different *Drosophila-Wolbachia* associations. Genetics 164: 545–552.
23. Werren JH (1997) Biology of *Wolbachia*. Annu Rev Entomol 42: 587–609.
24. Bressac C, Rousset F (1993) The reproductive incompatibility system in *Drosophila-simulans*: DAPI-staining analysis of the *Wolbachia* symbionts in sperm cysts. J Invertebrate Pathol 61: 226–230.
25. Presgraves DC (2000) A genetic test of the mechanism of *Wolbachia*-induced cytoplasmic incompatibility in *Drosophila*. Genetics 154: 771–776.
26. Snook RR, Cleland SY, Wolfner MF, Karr TL (2000) Offsetting effects of *Wolbachia* infection and heat shock on sperm production in *Drosophila simulans*: Analyses of fecundity, fertility and accessory gland proteins. Genetics 155: 167–178.
27. Boyle L, O'Neill SL, Robertson HM, Karr TL (1993) Interspecific and intraspecific horizontal transfer of *Wolbachia* in *Drosophila*. Science 260: 1796–1799.
28. Bordenstein SR, Werren JH (1998) Effects of A and B *Wolbachia* and host genotype on interspecies cytoplasmic incompatibility in *Nasonia*. Genetics 148: 1833–1844.
29. Sinkins SP, Walker T, Lynd AR, Steven AR, Makepeace BL, et al. (2005) *Wolbachia* variability and host effects on crossing type in *Culex* mosquitoes. Nature 436: 257–260.
30. Clark ME, Veneti Z, Bourtzis K, Karr TL (2002) The distribution and proliferation of the intracellular bacteria *Wolbachia* during spermatogenesis in *Drosophila*. Mechan Dev 111: 3–15.
31. Feder ME, Karr TL, Yang W, Hoekstra JM, James AC (1999) Interaction of *Drosophila* and its endosymbiont *Wolbachia*: Natural heat shock and the overcoming of sexual incompatibility. Am Zool 39: 363–373.
32. Karr TL, Yang W, Feder ME (1998) Overcoming cytoplasmic incompatibility in *Drosophila*. Proc R Soc Lond B Biol Sci 265: 391–395.
33. Sinkins SP, Braig HR, Oneill SL (1995) *Wolbachia* superinfections and the expression of cytoplasmic incompatibility. Proc R Soc Lond B Biol Sci 261: 325–330.
34. Andersson SG, Alsmark C, Canback B, Davids W, Frank C, et al. (2002) Comparative genomics of microbial pathogens and symbionts. Bioinformatics 18 (Suppl 2):: S17.
35. Moran NA, Plague GR (2004) Genornic changes following host restriction in bacteria. Curr Opin Genet Dev 14: 627–633.
36. Bordenstein SR, Reznikoff WS (2005) Mobile DNA in obligate intracellular bacteria. Nat Rev Microbiol 3: 688–699.
37. Wright JD, Sjostrand FS, Portaro JK, Barr AR (1978) The ultrastructure of the *Rickettsia*-like microorganism *Wolbachia pipientis* and associated virus-like bodies in the mosquito *Culex pipiens*. J Ultrastruct Res 63: 79–85.
38. Cohen AJ, Williamson DL, Oishi K (1987) SpV3 viruses of *Drosophila* spiroplasmas. Isr J Med Sci 23: 429–433.
39. van der Wilk F, Dullemans AM, Verbeek M, van den Heuvel JF (1999) Isolation and characterization of APSE-1, a bacteriophage infecting the secondary endosymbiont of *Acyrthosiphon pisum*. Virology 262: 104–113.
40. Wu M, Sun LV, Vamathevan J, Riegler M, Deboy R, et al. (2004) Phylogenomics of the reproductive parasite *Wolbachia pipientis* wMel: A streamlined genome overrun by mobile genetic elements. PLoS Biol 2: e69. DOI: 10.1371/journal.pbio.0020069
41. Masui S, Kuroiwa H, Sasaki T, Inui M, Kuroiwa T, et al. (2001) Bacteriophage WO and virus-like particles in *Wolbachia*, an endosymbiont of arthropods. Biochem Biophys Res Commun 283: 1099–1104.
42. Fujii Y, Kubo T, Ishikawa H, Sasaki T (2004) Isolation and characterization of the bacteriophage WO from *Wolbachia*, an arthropod endosymbiont. Biochem Biophys Res Commun 317: 1183–1188.
43. Masui S, Kamoda S, Sasaki T, Ishikawa H (2000) Distribution and evolution of bacteriophage WO in *Wolbachia*, the endosymbiont causing sexual alterations in arthropods. J Mol Evol 51: 491–497.
44. Bordenstein SR, Wernegreen JJ (2004) Bacteriophage flux in endosymbionts (*Wolbachia*): Infection frequency, lateral transfer, and recombination rates. Mol Biol Evol 10: 1981–1991.
45. Sanogo YO, Dobson SL (2004) Molecular discrimination of *Wolbachia* in the *Culex pipiens* complex: Evidence for variable bacteriophage hyperparasitism. Insect Mol Biol 13: 365–369.
46. Tram U, Ferree PA, Sullivan W (2003) Identification of *Wolbachia*-host interacting factors through cytological analysis. Microbes Infect 5: 999–1011.
47. Sanogo YO, Dobson SL (2006) WO bacteriophage transcription in *Wolbachia*-infected Culex pipiens. Insect Biochem Mol Biol 36: 80–85.
48. Iturbe-Ormaetxe I, Burke GR, Riegler M, O'Neill SL (2005) Distribution, expression, and motif variability of ankyrin domain genes in *Wolbachia pipientis*. J Bacteriol 187: 5136–5145.
49. Sanogo YO, Eitam A, Dobson SL (2005) No evidence for bacteriophage WO orf7 correlation with *Wolbachia* induced cytoplasmic incompatibility in the *Culex pipiens* complex (Culicidae: Diptera). J Med Entomol 42: 789–794.
50. Duron O, Fort P, Weill M (2006) Hypervariable prophage WO sequences describe an unexpected high number of *Wolbachia* variants in the mosquito *Culex pipiens*. Proc R Soc Lond B Biol Sci 273: 495–502.
51. Bordenstein SR, Uy JJ, Werren JH (2003) Host genotype determines cytoplasmic incompatibility type in the haplodiploid genus *Nasonia*. Genetics 164: 223–233.
52. Perrot-Minnot MJ, Guo LR, Werren JH (1996) Single and double infections with *Wolbachia* in the parasitic wasp *Nasonia vitripennis*: Effects on compatibility. Genetics 143: 961–972.
53. Lunde M, Blatny JM, Kaper F, Nes IF, Lillehaug D (2000) The life cycles of the temperate lactococcal bacteriophage phiLC3 monitored by a quantitative PCR method. FEMS Microbiol Lett 192: 119–124.
54. Ijichi N, Kondo N, Matsumoto R, Shimada M, Ishikawa H, et al. (2002) Internal spatiotemporal population dynamics of infection with three *Wolbachia* strains in the adzuki bean beetle, *Callosobruchus chinensis* (Coleoptera : Bruchidae). Appl Environ Microbiol 68: 4074–4080.
55. Kondo N, Ijichi N, Shimada M, Fukatsu T (2002) Prevailing triple infection with *Wolbachia* in *Callosobruchus chinensis* (Coleoptera : Bruchidae). Mol Ecol 11: 167–180.
56. Mcgarry HF, Egerton GL, Taylor MJ (2004) Population dynamics of *Wolbachia* bacterial endosymbionts in *Brugia malayi*. Mol Biochem Parasitol 135: 57–67.
57. Hogge MAF, King PE (1975) The ultrastructure of spermatogenesis in *Nasonia vitripennis*. J Submicrosc Cytol Pathol 7: 81–96.
58. Binnington KC, Hoffmann AA (1989) *Wolbachia*-like organisms and cytoplasmic incompatibility in *Drosophila simulans*. J Invertebrate Pathol 54: 344–352.
59. Dudkina NV, Kiseleva EV (2005) [Structural organization and distribution of the symbiotic bacteria *Wolbachia* during spermatogenesis of *Drosophila simulans*]. Ontogenes 36: 41–50.
60. Liu BL, Everson JS, Fane B, Giannikopoulou P, Vretou E, et al. (2000) Molecular characterization of a bacteriophage (Chp2) from *Chlamydia psittaci*. J Virol 74: 3464–3469.
61. Masui S, Sasaki T, Ishikawa H (2000) Genes for the type IV secretion system in an intracellular symbiont, *Wolbachia*, a causative agent of various sexual alterations in arthropods. J Bacteriol 182: 6529–6531.
62. Foster J, Ganatra M, Kamal I, Ware J, Makarova K, et al. (2005) The *Wolbachia* genome of *Brugia malayi*: Endosymbiont evolution within a human pathogenic nematode. PLoS Biol 3: e121. DOI: 10.1371/journal.pbio.0030121
63. Barnett V, Lewis T (1994) Outliers in statistical data. New York: Wiley. 604 p.
64. Osborne JW, Overbay A (2004) The power of outliers (and why researchers should always check for them). Pract Assess Res Eval 9: 1–10.
65. Sokal RR, Rohlf FJ (1981) Biometry. New York: WH Freeman and Company. 857 p.